Proceedings of the 5th WSEAS Int. Conf. on Power Systems and Electromagnetic Compatibility, Corfu, Greece, August 23-25, 2005 (pp534-538)

The Linear Switched Reluctance Actuator Functional Performance. A Basis to the Effectiveness on Control Design.

Maria R. A. Calado, António E. Espírito-Santo, Carlos M. P. Cabrita
Department of Electromechanical Engineering
University of Beira Interior
Calçada Fonte do Lameiro, 6201-001 Covilhã
PORTUGAL

Abstract: - This paper presents a new procedure, based on experimental obtained results, to characterise a built 6 primary and 4 secondary Linear Switched Reluctance Actuator (LSRA), concerning the main performance characteristics. This actuator is a part of a complete electrical drive developed by the authors in the Electrical Machines and Power Electronics Lab of the University of Beira Interior, to be applied in a machine-tool [1,2]. The knowledge of a chosen set of obtained characteristics allows the control designer to proper feed the actuator, for pre-defined mover relative positions, and for coil current excitation levels that brings the machine to desired functional performances, according to different practical applications tasks.

Key-Words: - Linear Switched Reluctance Actuator, Design, Analysis and Construction, FEA, Experimental Characteristics.

1 Introduction

The linear switched reluctance actuators (LSRA) are counterparts of rotary SRMs, that is the linear configuration can be obtained to result from the rotary configuration, i.e., cut radially and unrolled. Thus, the LSRA develops force (thrust) and motion by the tendency of a secondary to assume a position where the inductance of the dc excited primary is maximised [1,2].

This kind of linear electric machine is not compatible with machine conventional design methodologies. In fact, the classical empirical parameters used in those approaches are, in this case, unknowns, as well as the magnetic flux density distribution and, consequently the actuator performance [3,4].

The always different machine topology, for different relatives positions between primary and secondary, relieve the actuator design out of strictly analytical analysis. The finite element method (FEM) for numerical analysis of this kind of non--conventional machine is an important tool for models simulation. FEM allows the magnetic characteristics knowledge, as magnetic co-energy variation W_c , and magnetic energy variation W , for different relative positions between primary and secondary parts, x.

This paper concerns the actuator performance characterization, based on both already proposed and performed design, and analysis methodology, [3]–[7], and on obtained experimental characteristics of a constructed linear switched reluctance actuator prototype. That prototype has construction data and electrical parameters listed in Appendix.

Possibilities for actuator applications are numerous, for different physical configurations, with proper relative positions for primary coils excitation and interfering in current levels. Thus, the knowledge of these functional characteristics makes possible the choice, and establishment, of proper control methodology.

2 Machine Design

For linear switched reluctance actuators the optimised design consists to obtain the best performances in terms of current and forces with a minimum of construction materials volume and weight (magnetic iron and copper), that is to obtain the best specific force – longitudinal force or thrust to machine weight ratio. As already told, it is not possible to adopt conventional machine design procedures for this kind of non-conventional machines.

Thus, the author's opinion is that the design should follow three steps, as stated in [3,7], that are: the specification of main data, with main electrical and mechanical requirements, as are the rated thrust up to the base speed F, the base speed V, the dc link voltage V_0, the number of phases, m and the

topology (tubular or flat); the analytical calculus, following a logic sequence to calculate electrical and mechanical parameters (performed by computer programs, changing and adapting different parameters, in order to obtain the required actuator performance, established by the designer), as for example with the teeth slots and airgap dimensional parameters, thrust and current densities F_x and J, turn on and off positions x_i and x_o, and slot fill, safety and saturated factors; and the numerical analysis, being possible the determination of the effect of geometry changing, or the influence of excitation positions and current levels, in machine performance.

Described design points procedure were presented by author's in [8,9], and were the basis for the prototype construction (shown in Fig. 1), wich performance is here under analysis.

Figure 1 LSRA prototype mounted on the test rig

Some important dimensional and design adoptions must be refereed, in order to better expose actuator construction procedures:

2.1 Actuator Analytical Design

The adopted design method is based on the following calculus:

$$x_a - x_i \approx 0.8\, b_p \tag{1}$$

where x_a is the aligned position, x_i the turn-on position and b_p the primary tooth width; primary and secondary stack width is given by:

$$w = \frac{F}{2 b_p F_x} \tag{2}$$

where F_x is the thrust density; the number of turns per coil is:

$$N_1 = \frac{V_0}{V}\frac{(x_a - x_i)}{2\, b_p w\, B_g}, \tag{3}$$

where B_g is the maximum airgap flux density; the unsaturated inductances for the aligned and the unaligned position are:

$$L_{an} = 2\mu_0 N_1^2 \frac{w b_p}{g} \text{ , and } L_{na} = \frac{L_{an}}{10} \tag{4}$$

where g is the airgap length and μ_0 the free space magnetic permeability; the primary slot is given by:

$$h_p = \frac{2 N_1 I_c}{c_p k_e J}, \tag{5}$$

where c_p is the primary slot width and J the conductor current density; the secondary tooth depth is calculate by:

$$h_s = (20...30) g\,; \tag{6}$$

the primary and secondary yoke thickness are:

$$n_p\,(\text{or } n_s) = (0.60...0.70)\, b_p\,(\text{or } b_s) \tag{7}$$

with primary and secondary heights:

$$H_p = h_p + n_p\,; H_s = h_s + n_s\,; \tag{8}$$

the winding conductor diameter is giving by:

$$d_{Cu} = 2\sqrt{k_e c_p h_p / 2\pi N_1}\,, \tag{9}$$

where k_e is the slot fill factor; the mean coil length is:

$$L_1 = 2w + 1.2\pi b_p\,, \tag{10}$$

Concerning the excitation current *I*, and the traction developed force *F* for this kind of machine one has, respectively, that:

$$F(i,x) = \frac{\partial W_c(i,x)}{\partial x} \tag{11}$$

$$W_c = k_c\left[(\psi_c - L_{na} I_c) k_t I_c - \frac{(\psi_c - L_{na} I_c)^2 k_t^2}{2 L_{an}}\right] \tag{12}$$

where k_c is the safety factor, k_t the duty-cycle factor, ψ_c and W_c respectively the peak flux linkage per phase during a conducting period at a constant speed and the area in the energy cycle, given by $\psi_c = (V_0/V)(x_a - x_i)$ and $W_c = k_t b_p F$ [2].

2.2 Actuator Numerical Design

The Finite Element Method (FEM) is now a popular method and are commonly used in Electrical Engineering, namely for the analysis of electromagnetic phenomenon's. This method, and the corresponding existing software packages based on it, provides a number of benefits, as are the performance optimisation of electromagnetic devices and the reduced investment, in both better performance/material ratio and decreasing on build prototypes [9]. In addition, and concerning this particular actuator, after prototype construction, the FEM is a major method for performance analysis, with the possibilities of change excitation positions and current levels. It is possible to considerer different dimensional parameters, as the airgap length or the pole tooth width, and investigate their influence on magnetic airgap flux, or in the traction force. It is even possible to recognize construction difficulties and calculate necessary material costs.

Behind these optimisation philosophies, one can considerer the performance prediction, allowing the knowledge of proper currents and positions, and by this way direct interfere in control approaches.

Figure 2 shows a possible utilization of this kind of analysis, evaluating, in this example, the influence of different airgap length on the distribution of magnetic flux density, being also possible to know the critical points where saturations can occur.

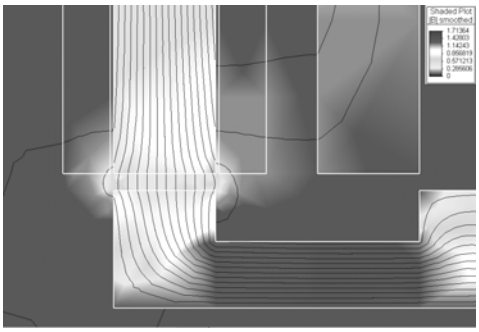

Figure 2 Distribution of magnetic flux density for the aligned position

3 Functional Performance Evaluation

Taking into account the simulated obtained characteristics, trough the application of FEM, the machine prototype was submitted to experimental tests.

Within various obtained characteristics, here one discusses the application of two sets of characteristics, that can proper define procedures, and are an adequate basis, for the control design: (1) the maximum current characteristics and (2) the corresponding maximum traction force characteristics.

The machine primary (mover), with one elementary element (6 phases), was installed between two rails in a test rig, being the secondary part of the machine build with 5 elementary elements. One load cell, with a complete measumerement aquisiction system, was connected in the primary part of the machine.

The test rig was been built allowing the primary to be locked in specific relatives positions, in order to proper know the stactic forces along the machine length. The test rig was even capable to keep mechanical distance between primary and secondary (experimental traction test were made for different airgap lengths). For each position, the excitation constant current, i, was been changed within proper limits [7].

The current limits were established either by previously performed heating test (establishes the rated current and the overload current-time characteristic) and by mechanical limitations. In fact, the simulated current levels (from 0 to 10 A), used to investigate magnetical characteristics, and saturation occurrences, through finite element method (FEM), were in pratice only possibles for limited time, and according to obtained current-time characteristic.

Concerning the mechanical limitations, some of the simulated current were not possible to be tested, avoiding physical contact between primary and secondary, due to the extremealy high atraction forces.

Figure 3 shows the coil current limitation excitation envelopes, before secondary levitation due to magnetic attraction force (this force is high enough to compensate the machine eight, I_{lev}, for different secondary relative positions, between the unaligned left position and the unaligned right position, with an incremental step of 5 mm, and for excitation currents varying from 0.5 to 5 A, with incremental step of 0.1 A, for a proposed configuration, and for different airgap lengths

(g = 2 mm, the most minimum advisable airgap for this machine, g =4 mm and g = 8 mm).

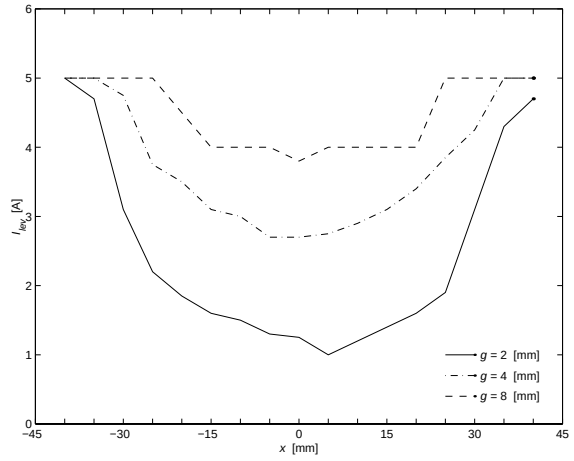

Figure 3 Characteristics of primary maximum current, I_{lev}, before the occurrence of secondary levitation, for different relative positions and for different airgap lengths

Figure 4 shows the traction force envelopes possibilities, F_{lev}, for different secondary relative positions, and for different airgap lengths, the same as those of Fig. 3. Positive and negative force values correspond to right and left secondary movements.

Note that only some of the acquired values are shown, in order to have a better figure understanding.

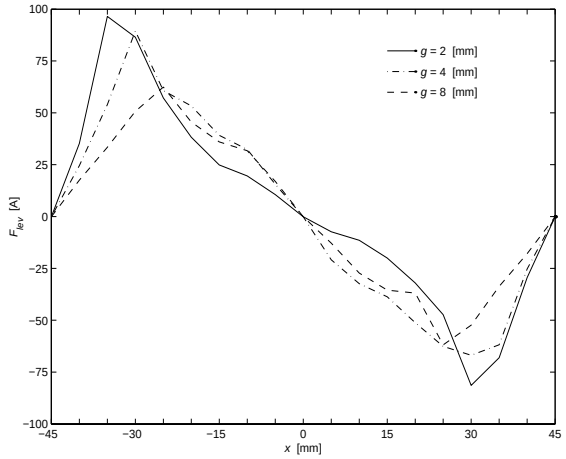

Figure 4 Characteristics of maximum traction force, F_{lev}, before the occurrence of secondary levitation, for different relative positions and for different airgap lengths

These characteristics show all possible combinations of pairs (x,I), being x the relative secondary position and I the excitation current level.

That is, the areas under shown curves represent the position/excitation possibilities, and correspond to traction forces possibilities, for each actuator configuration (different airgap length).

Through the referred characteristics analysis is possible to choose suitable pairs (x,I) for different practical applications, as transportation systems (actuator with small thrust values, but with smooth movement), or stroke systems (actuator with considerable thrust values). The actuator with 2 mm airgap length is a very powerful machine, from the ability of traction force development point of view, being however extremely irregular this ability along the movement, for the different secondary relative positions. The adoption of an actuator with this performance nature imposes the feeding of coils in precise relative positions, as the beginning, or very close positions, of pole/phase alignment; this way, the next phase coil to be excited must achieve his one optimum position as a result of one single impulse in previous fed phase. This is a more demanding actuator for control of force ripple minimization proposes.

On the other hand, actuators with larger airgap lengths are less attractive for traction force development, but are suitable for applications demanding smooth movement, with traction force adaptation for different positions (can be obtained controlling the coil excitation current level).

The analysis of Figs. 3 and 4 also shows a small unbalance between tested teeth. That fact is observed for equivalent positions around the alignment position, and being the traction forces lower for positions corresponding to the abandonment of refereed position, and characterised by forces stipulated as negative, i.e. forces that make actuator move in opposite direction. Thus, the actuator is unable to develop the same traction force values if the tendency of movement is that one to positions when the primary is more and more close to the secondary edge, with higher leakage flux.

4 Conclusion

The aim of this work is to contribute for the LSRA understanding and characterisation, given guidance for control design methodology, taking into account different practical applications. The definition of both proper coils excitation positions together with proper current level, in order to optimise the traction mechanical force and system efficiency is the basis

for next control approach.

Being the analysed actuator of great complexity, without physical symmetries along his movement, and presenting local and global saturation variations, that are preponderant for actuator performance, the better knowledge of performance characteristics tends to give a considerable easiness to control analysis and design.

References:

[1] Boldea, I. and Nasar, S. A., *Linear Electric Actuators and Generators*, Cambridge University Press. 1997, Cambridge, UK.

[2] Miller, T. J. E., *Switched Reluctance Motors and their Control*, Magna Physics Publishing and Oxford Science Publications. 1993, Oxford, UK.

[3] Calado, M. R., Actuador Linear de Relutância Variável Comutado. Modelização, Dimensionamento, Construção e Ensaio, *PhD Thesis (in Portuguese)*, July 2002, Universidade da Beira Interior, Covilhã, Portugal.

[4] Calado, M. R., Gonçalves, J. G. and Cabrita, C. P., Design of a Linear Switched Reluctance Actuator. Analytical and Numerical Analysis, *Proceedings of the Symposium on Power Electronics, Electrical Drives, Automation and Motion*, pp.C3-7–C3-11, 11-14 June 2002, Ravello, Italy.

[5] Calado, M. R. and Cabrita, C. P., The Linear Switched Reluctance Actuator (in Portuguese), *Electricidade Journal*. Lisbon, no. 358, September 1998, pp.206-213.

[6] Calado, M. R., Cabrita, C. P., Aspectos Complementares de Análise e Dimensionamento de Motores e Actuadores de Relutância Variável Comutados. *Electricidade Journal* (in Portuguese), Nº. 392, Jan-Fev 2002, pp.13-22. Lisbon, Portugal.

[7] Calado, M. R., Cabrita, C. P., A New Linear Switched Reluctance Actuator: Performance Analysis, *Proceedings of the Fourth International Symposium on Linear Drives for industry Applications*, 8-10 September 2003, Birmingham, UK.

[8] M. R. A. Calado, C. Pereira Cabrita, "Traction Forces in Linear Reluctance Actuators", *Proceedings of the 8th Luso-Spanish Conference of Electrotechnic Engineering – 8º. CLEE*, Vilamoura, Portugal, 3-5 July 2003.

[9] M. R. A. Calado, C. M. P. Cabrita, "Finite Elements Method in Electromagnetism for Actuator Design And Dynamic Behavior Prediction", *Proceedings of the International Conference on Computational & Experimental Engineering and Sciences - ICCES 2004*, Funchal, Portugal, 26-29 July 2004.

APPENDIX

Analysed machine details:

Main data	
Rated thrust, F	250 N
Base speed, V	0.8 m/s
Dc link voltage, V_0	200 V
Number of phases, m	3
Topology	Flat
Thrust density, F_x	2 N/cm^2
Complementary data	
Primary tooth width, b_p	30 mm
Primary slot width, c_p	30 mm
Secondary tooth width, b_s	30 mm
Secondary tooth height, c_s	60 mm
Primary slot pitch, τ_p	60 mm
Secondary slot pitch, τ_s	90 mm
Airgap length, g	0.5 mm
x_0-x_i	24 mm
Conductor current density, J	3.5 A/mm^2
Slot fill factor, k_e	0.4
Safety factor, k_c	0.7
Duty-cicle factor, k_t	1.0
Calculated data	
Primary length, L	330 mm
Primary/secondary stack width, w	104 mm
Primary slot depth, h_p	89 mm
Secondary tooth depth, h_s	15 mm
Primary height, H_p	108 mm
Secondary height, H_s	35 mm
Number of turns per coil, N_1	640
Mean coil length, L_1	322 mm
Winding conductor diameter, d_{Cu}	1 mm
Current per phase, I_c	5 A
Efficiency, η	48.3 %